Preprints.org

Article

Not peer-reviewed version

Advanced Electrochemical Degradation of Organic Pollutants From Water Using Sb-Doped SnO2/Ti Anode and Assisted by Granular Activated Carbon

Anamaria Baciu , Corina Orha , Radu Nicolae , Mircea Nicolaescu , Sorina Ilies , Florica Manea *

Posted Date: 31 May 2023

doi: 10.20944/preprints202305.2190.v1

Keywords: advanced water treatment; electrochemical filtering; doxorubicin; mesoporous Sb-doped SnO2 electrode; activated carbon; particulate electrode

Preprints.org is a free multidiscipline platform providing preprint service that is dedicated to making early versions of research outputs permanently available and citable. Preprints posted at Preprints.org appear in Web of Science, Crossref, Google Scholar, Scilit, Europe PMC.

Copyright: This is an open access article distributed under the Creative Commons Attribution License which permits unrestricted use, distribution, and reproduction in any medium, provided the original work is properly cited.

Preprints (www.preprints.org) | NOT PEER-REVIEWED | Posted: 31 May 2023 doi:10.20944/preprints202305.2190.v1

Disclaimer/Publisher's Note: The statements, opinions, and data contained in all publications are solely those of the individual author(s) and contributor(s) and not of MDPI and/or the editor(s). MDPI and/or the editor(s) disclaim responsibility for any injury to people or property resulting from any ideas, methods, instructions, or products referred to in the content.

Article

Advanced Electrochemical Degradation of Organic Pollutants from Water Using Sb-Doped SnO_2/Ti Anode and Assisted by Granular Activated Carbon

Anamaria Baciu [1], Corina Orha [2], Radu Nicolae [1], Mircea Nicolaescu [1,2], Sorina Ilies [3] and Florica Manea [1,*]

[1] Department of Applied Chemistry and Engineering of Inorganic Compounds and Environment, Politehnica University of Timisoara, Blv. Vasile Parvan No. 6, 300223, Timisoara, Romania; anamaria.baciu@upt.ro (A.B.); florica.manea@upt.ro (F.M.); radu.nicolae@student.upt.ro (R.N.) mircea.nicolaescu@student.upt.ro (M.N.),

[2] National Institute for Research and Development in Electrochemistry and Condensed Matter, Timisoara, Condensed Matter Department, 1 P. Andronescu Street, 300254, Timisoara, Romania; orha.corina@gmail.com (C.O.), mircea.nicolaescu@student.upt.ro (M.N.)

[3] "Coriolan Drăgulescu" Institute of Chemistry, Romanian Academy, 24 Mihai Viteazu Bvd., 300223 Timisoara, Romania, sorinailies@acad-icht.tm.edu.ro

* Correspondence: florica.manea@upt.ro

Abstract: In this paper, mesoporous electrodes consisted of Sb-doped SnO_2 deposited onto Ti plates controlled corroded under acidic medium were synthesized by spin-coating method, and morpho structurally characterized by X-ray diffraction (XRD) and scanning electron microscopy (SEM). The electrodes were electrochemical testing in the degradation/mineralization by electrooxidation (EO) of doxorubicin (DOX) as single-component and multi-component together with capecitabine (CCB)-from cytostatic class and humic acid (HA)-from natural organic matter (NOM) class in the absence/the presence of activated carbon (AC) as particulate electrode. The best mineralization efficiency of 67 % was achieved for DOX mineralization using Sb-doped SnO_2 deposited onto Ti plate controlled corroded with oxalic acid in electrooxidation process. The presence of AC within the electrolysis process generated a synergy effect of 52.75 % for TOC parameter removal, which is in accordance and quite better than the result reported in the literature. The aspects related to the complex mechanism of DOX degradation and mineralization are discussed. The superiority of AC assisted electrooxidation, as electrochemical filtering (EF), was proved considering simultaneous degradation and mineralization of mixture of doxorubicin, capecitabine and humic acid.

Keywords: advanced water treatment; electrochemical filtering; doxorubicin; mesoporous Sb-doped SnO_2 electrode; activated carbon; particulate electrode

1. Introduction

The presence of pharmaceuticals in water is continuously growing and should exhibit the possible negative effects on the ecology status of the surface water in both the short and long term, one of the main sources being industrial pharmaceuticals wastewaters. Cytostatic drugs are classified as hazardous waste due to their carcinogenic, teratogenic, and mutagenic properties with very negative impact on the water quality and the human health.

Considering their xenophobic and refractory character, the researchers for their removal are focused on the application of advanced oxidation processes (AOPs), which are based on in-situ production of hydroxyl radical (·OH) for their mineralization [1,2]. Among the AOPs, electrochemical advanced oxidation processes (EAOPs) have been extensively studied for treating various types of pharmaceutical wastewaters, due to their high versatility, efficiency, and environmental compatibility [1].

© 2023 by the author(s). Distributed under a Creative Commons CC BY license.

Preprints (www.preprints.org) | NOT PEER-REVIEWED | Posted: 31 May 2023 doi:10.20944/preprints202305.2190.v1

Considering the key role of the electrode in the performance of the electrochemical processes, various types of electrodes, such as: graphite [3], platinum (Pt) [4], carbonaceous matrix, boron doped diamond (BDD) [5] and dimensionally stable anodes (DSA) [6,7] have been studied.

Dimensionally stable electrodes (DSA) consisted of metal-oxide films deposited on titanium or other substrates and have been used to replace the conventional electrodes in advanced wastewater treatment [6]. DSA electrodes have been widely investigated in the field of water electrolysis, electro chlorination, cathodic protection, wastewater treatment [7] due to their advantages regarding stable size, long service life, high electrocatalytic activity, and low cost [8]. They have large specific surface area, desired mechanical and chemical properties, *e.g.*, good stability, low resistivity, and excellent resistance to corrosion at high currents [9]. Typically, Ti foil is used as the substrate, and the primary chemical composition of the coating is transition metal oxide, *e.g.*, RuO_2, IrO_2, TiO_2, SnO_2, PbO_2, MnO_2, and Ta_2O_5. DSA exhibit high electroactive surface areas due to their mud-cracked like morphology, allowing the direct oxidation of organic pollutants on the electrode surface at low potentials and are able to promote the formation of active intermediates (Cl_2, ClO^-, $OH\cdot$, O_3) to perform the indirect oxidation of pollutants [10].

Antimony-doped tin dioxide deposited onto Ti substrate (Ti/SnO_2-Sb) electrode is considered as one of the most promising DSA type anode materials used for electrooxidation process in wastewater treatment due to its advantages of relatively high oxygen evolution potential (OERP), high electrooxidation activity, low cost, and low toxicity [11–14]. Several synthesis methods have been reported for its preparation, *e.g.*, dip-coating [15], electrolytic deposition [16], spin coating [17] and pyrolysis spray [18].

Usually, a traditional two-dimensional (2D) electrode reactor is commonly used for electrochemical process including advanced electrooxidation, but there are some disadvantages, *e.g.*, small electrode surface area, low current efficiency, limited mass transfer, temperature rise during processing, and short lifetime of electrodes [19].

Recently, 3D electrochemical process has attracted much attention because of its unique properties and advantages, regarding the high current efficiency and the high space–time yield. It is well-known that 3D electrochemical process is similar to 2D electrochemical process, except the porous surface of the anode and/or the presence of the third electrode named particulate electrode [20]. Properties including high specific area for good adsorption capacity, high electrocatalytic activity, and stability for the coating substrate or good conductivity that can increase the current efficiency are required for good particulate electrode materials. Granular activated carbon (AC) has been tested as composition of the particulate electrode for enhancing the efficacy of the electrochemical system in various wastewater treatments [21–23]. The pollutant degradation is improved due to the AC particles under voltage applying becoming the micro-electrolysis cells, which are able to generate hydrogen peroxide and subsequent, the hydroxyl radicals [21,24–27]. Also, AC exhibits the sorption ability for many types of pollutants enhancing the mass transfer and as consequence, the higher pollutant degradation efficiency [28].

Considering our previously reported results achieved for the degradation and mineralization of doxorubicin (DOX), a common cytostatic used for cancer therapy, which can be found in water, using Ti-based SnO_2 anode in electrooxidation process with a maximum electrochemical mineralization efficiency of 0.147 mg C/C·cm^2 [29], this work aims to enhance the electrochemical performance for DOX degradation and mineralization. Two approaches are considered, one is to improve the anode properties by its composition and morphology and the other is to introduce granular activated carbon as particulate electrode. The synthesis by spin-coating method of the mesoporous Sb-doped SnO_2 onto controlled corroded Ti plates, their characterization and electrochemical testing are studied for the degradation/mineralization of DOX as single-component and multi-component together with capecitabine (CCB)-from cytostatic class and humic acid (HA)-from natural organic matter (NOM) class in the absence/the presence of AC as particulate electrode.

Preprints (www.preprints.org) | NOT PEER-REVIEWED | Posted: 31 May 2023 doi:10.20944/preprints202305.2190.v1

2. Materials and Methods

2.1. DSA electrode synthesis

A three-stage procedure involving titanium substrate pretreatment, precursor reagent preparation, sol-gel spin coating/ dip coating subsequent calcination process was used to form an SnO_2-Sb coating on Ti substrates to obtain Ti/SnO_2-Sb electrodes (Figure 1).

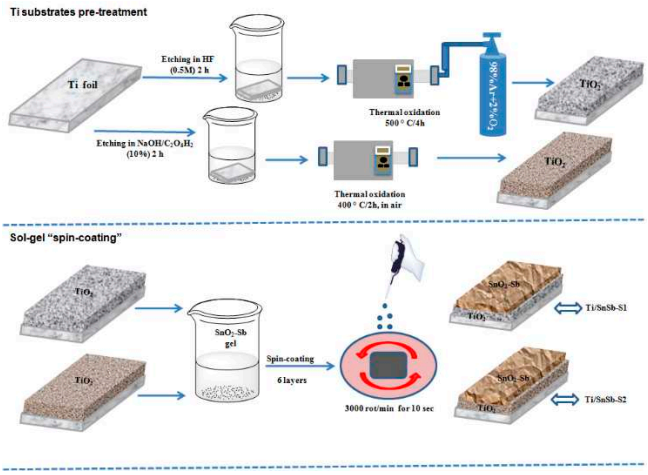

Figure 1. Schematic diagram of preparation of Ti/SnO_2-Sb electrodes.

First, Ti substrates (2.5 X 2.5 cm), were operated successively by polishing, degreasing and etching in oxalic acid (10 %) as our previous work [29]. Another way to etching the Ti plate wase the fluorhidric acid (0.5 M), for 2h. For the formation of crystalline TiO_2, the process of thermal oxidation was carried out in a tubular furnace in a controlled atmosphere consisting of a mixed gas flow of Ar and O_2 at a temperature of 500°C for 4 h.

Ti/SnO_2-Sb electrodes were prepared by spin-coating method using corroded Ti plate and uncorroded Ti plate. Thus, Sb doped SnO_2 was deposited onto Ti plate corroded with HF (Ti/SnSb-S1) and respectively with oxalic acid (Ti/SnSb-S2). For comparison, Sb doped SnO_2 was deposited onto uncorroded Ti plate (Ti/SnSb-S0).

The preparation process consisted of $SnCl_4$, $SbCl_3$ with molar ration of Sn:Sb = 1.00:0.1 were dissolved in ethanol, Pluronic P-123, water mixed solution for 4 h. This transparent gel was left standing to age at least 24 hours at 60ºC before coating. Ti/SnO_2-Sb electrodes were achieved by spin-coating method (WS-400-6NPPB Spin Coater-Laurell Technology Corporation) by deposition of 6 layers of SnO_2-Sb thin films on Ti plates, according to the protocol described in our previous work [29].

2.2. Physicochemical characterization

The crystalline structure of the Ti/SnO_2-Sb electrodes was characterized by X-ray diffraction (XRD, PANalytical X'Pert PRO MPD Diffractometer, Almelo, The Netherlands) with Cu-Kα radiation (λ= 1.5418 Å) in the range 2θ = 10–80°. The morphology of the layers was examined using scanning electron microscopy (SEM, FEI Inspect S model, Eindhoven, The Netherlands).

2.3. Electrochemical characterization and degradation

The electrochemical characterizations and testing of the Ti/SnO_2-Sb electrodes were performed by cyclic voltammetry (CV) and chronoamperometry (CA) using the classical three-electrode cell system and GPES 4.9 software controlled Autolab potentiostat/ galvanostat PGSTAT 302 (Eco Chemie, The Netherlands). The three-electrode cell system consisted of saturated calomel reference electrode (SCE), a platinum plate counter electrode, and Ti/SnO_2-Sb working electrode, considering all types of above-presented antimony-doped tin oxides coated onto un-corroded/corroded Ti

Preprints (www.preprints.org) | NOT PEER-REVIEWED | Posted: 31 May 2023 doi:10.20944/preprints202305.2190.v1

substrates (Ti/SnSb-S0-S2 electrodes). The electrochemical testing of all three electrodes was carried out in the degradation and mineralization of doxorubicin (DOX), a cytostatic considered as emerging pollutant in water. Also, for optimal conditions, the degradation and mineralization of mixture of doxorubicin (DOX), capecitabine (CCB) as another commonly used cytostatic and humic acid (HA) as main component of natural organic matter (NOM) was assessed.

DOX, CCB and HA concentrations were determined based on UV-VIS spectra recorded with Agilent Cary 100 UV/VIS spectrophotometer (California, United States) at specific wavelengths. Spectrophotometrically, DOX concentrations were assessed at wavelengths of 486 nm, 290 nm, 253 nm, and 232 nm, CCB concentration was determined at the wavelengths of 302 nm, 240 nm and 213 nm and HA concentration at 254 nm. (Figure S1).

The organics degradation degree (η) and electrochemical degradation degree **(E_{org})** were determined based on equations (1) and (2):

$$\eta_{org} = \frac{(C_{org,i} - C_{org,f})}{C_{org,i}} \cdot 100 \ (\%) \quad (1)$$

$$E_{org} = \frac{(C_{org,i} - C_{org,f})}{C \cdot S} \cdot V \ (mg / C \cdot cm^2) \quad (2)$$

where: $C_{org,i} - C_{org,f}$ represents the change in the organics (DOX, CCB and HA) concentration, determined by spectrophotometry at each absorbance during electrochemical experiments; *C is* charge consumption corresponding to various electrolysis time, *V* is the sample volume (20 cm^3) and *S* is the area of the electrode surface (3 cm^2).

Also, the organics mineralization degree (η_{TOC}) and electrochemical mineralization degree **(E_{TOC})** were determined considering the change in TOC concentration instead of organics concentration, based on equations (3) and (4):

$$\eta_{TOC} = \frac{(C_{TOC,i} - C_{TOC,f})}{C_{TOC,i}} \cdot 100 \quad (\%) \quad (3)$$

$$E_{TOC} = \frac{(C_{TOC,i} - C_{TOC,f})}{C \cdot S} \cdot V \ (mg / C \cdot cm^2) \quad (4)$$

Total organic carbon (TOC) parameter was analyzed using Shimadzu TOC analyzer (Columbia, Maryland, U.S.A.).

For a more accurate assessment of the mineralization process efficacy taking into account the energy consumption, the mineralization current efficiency (MCE) is determined in according with equation (5) [30]:

$$MCE = \frac{n\, F\, V_S\, \Delta(TOC)_{exp}}{4.32 \times 10^7 mIt} \cdot 100 \quad (\%) \quad (5)$$

where n is the number of electrons consumed in the mineralization process of DOX, F is the Faraday constant (= 96 487 C · mol^{-1}), V is the solution volume (dm^3), $\Delta_{(TOC)exp}$ is the experimental TOC decay (mg · dm^{-3}), 4.32 · 10^7 is a conversion factor for units homogenization (= 3 600 s h^{-1} · 12 000 mg of carbon mol^{-1}), m is the number of carbon atoms in organic, I is the applied current (A), and t is time (h). The number of electrons consumed is determined based on the overall mineralization reaction of organics to CO_2.

The mineralization reactions of organics are considered based on the equation (6) for DOX, (7) for HA and (8) for CCB:

$$DOX: C_{27}H_{29}NO_{11} + 46H_2O \rightarrow 27CO_2 + 121H^+ + NO_3^- + 120e^- \quad (6)$$

$$HA: C_9H_9NO_6 + 15H_2O \rightarrow 9CO_2 + NO_3^- + 39H^+ + 38e^- \quad (7)$$

$$CCB: C_{15}H_{22}FN_3O_6 + 33H_2O \rightarrow 15CO_2 + 88H^+ + F^- + 3NO_3^- + 84e^- \quad (8)$$

The energy consuming was assessed per gram of TOC removed (SEC) and per litre of the water treated (Wsp) using equation (9) and (10), respectively:

$$SEC = \frac{U \cdot I \cdot t}{(TOC_i - TOC_f)V} \quad (Wh \cdot g^{-1}\ TOC) \quad (9)$$

Preprints (www.preprints.org) | NOT PEER-REVIEWED | Posted: 31 May 2023 doi:10.20944/preprints202305.2190.v1

where: SEC is energy consumption, U is the cell voltage (V), I indicate the applied current (A), t is the electrochemical oxidation time (h), V is the volume of the cell (dm^3), TOC_i and TOC_f are the initial and final TOC concentration (mg C·dm^{-3}) at time t, respectively.

$$Wsp = \frac{U \cdot I \cdot t}{V} \quad (Wh \cdot dm^{-3}) \tag{10}$$

where U is the potential (V), I is the applied current (A), t is the electrolysis time (h), and V the volume of the treated solution (dm^3).

3. Results and Discussion

In the first stage, all electrodes of Sb doped SnO_2 deposited onto uncorroded/corroded Ti plates were characterized morpho-structurally by XRD and SEM.

3.1. Morphostructural characterization

The crystal structures of the electrodes were studied by using X-ray diffraction (XRD). Figure 2 shows that the diffraction peaks of the electrodes were observed at 2θ = 26.6º, 33.9º, and 51.8º, which were assigned to the (110), (101), and (211) planes of SnO_2. It is noticed that no peaks corresponding to antimony oxides were detected mostly because of trace amount of antimony added in sol–gel or because the element Sb might have entered into the lattice of SnO_2 crystal by substitution [31]. The precence of a few small Ti peaks at 2θ = 38.41º, 40.19º, 53.11º and 70.62º, which were assigned to the (002), (101), (102) and (103) planes indicates the existence of some cracks on the electrodes surface.

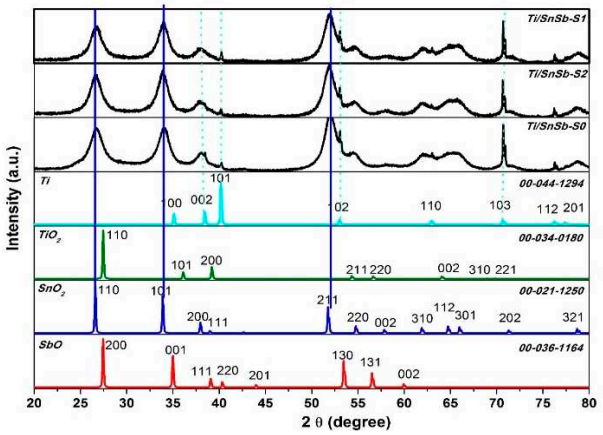

Figure 2. XRD spectra of the Ti/SnO_2-Sb electrode surfaces.

SEM photographs and energy dispersion spectra of the surface coating of the obtained electrodes are revealed in Figure 3, which illustrates the surface morphologies of the Ti/SnSb-S0, Ti/SnSb-S1 and Ti/SnSb-S2 electrodes.

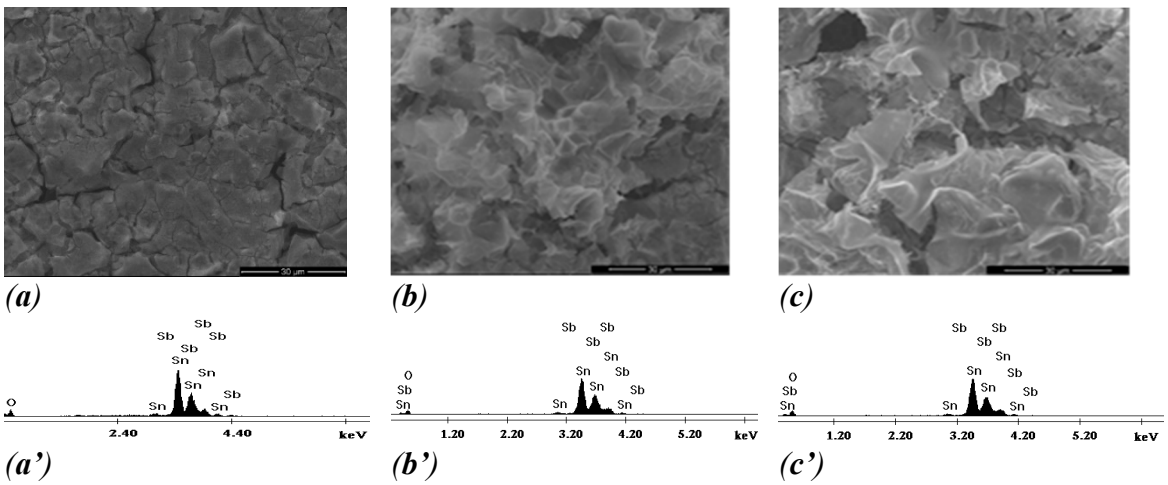

Preprints (www.preprints.org) | NOT PEER-REVIEWED | Posted: 31 May 2023 doi:10.20944/preprints202305.2190.v1

Figure 3. SEM images (a, b, c) and ED spectra (a', b' c') of Ti/SnSb-S0 (a, a'); Ti/SnSb-S1 (b, b') and Ti/SnSb-S2 (c, c') electrodes.

When the gel was deposited onto a non-corroded Ti plate, the compact morphology containing "mud-like cracks" which corresponds to classical 2-D smooth was observed. The phenomenon of "cracked-mud" production was assumed to the expansion properties between the Sn-Sb active layer and titanium substrate during calcinations process and the solvent evaporation [32]. It is well-known that during their application in the electrochemical processes, the penetration of electrolyte into the substrate through these cracks could mitigate the binding force between the film coating and the substrate, which would seriously affect the electrochemical activity and stability [33–35]. After coating corroded Ti plate with Sb-SnO_2 sol-gel precursor, the electrodes shows a more compact surface, proving that Ti corrosion in an acidic medium allowed obtaining a mesoporous surface characteristics to 3-D electrode surface.

3.2. Electrochemical characterization

Oxygen evolution reaction potential (OERP) and capacitive component as background current give information about oxygen evolution activity and the electroactive surface area of the electrode. It is well-known that oxygen evolution reaction is major side reaction during advanced electrooxidation, at the potential corresonding to the hydroxyl radicals generation in according with reactions (11) and (12):

$$2H_2O \rightarrow O_2 + 4H^+ + 4e^- \quad (11)$$

$$H_2O \rightarrow \cdot OH + H^+ + e^- \quad (12)$$

Considering the aqueous supporting electrolyte composition, within the anodic process, ozone, chlorine, and persulphate are generated besides hydroxyl radicals, based on reactions (13)-(16), which can act as oxidizing agent during electrolysis.

$$3H_2O \rightarrow O_3 + 6H^+ + 6e^- \quad (13)$$

$$2Cl^- \rightarrow Cl_2 + 2e^- \quad (14)$$

$$Cl_2 + H_2O \rightarrow HClO + Cl^- + H^+ \quad (15)$$

$$2SO_4{}^{2-} \rightarrow S_2O_8{}^{2-} + 2e^- \quad (16)$$

On the other hand, higher rate of oxygen evolution mitigates the current efficiency and increases the energy consumption. Also, the background current is direct proportional with the electroactive surface area, which is enhanced with the surface porosity increasing. The larger the electroactive surface area, the better the electrochemical activity of the electrode surface.

Cyclic voltammograms (CVs) were recorded in 0.1 M Na_2SO_4 solution, mixture of 0.05 M Na_2SO_4 and 0.05 M NaCl solution to evaluate the oxygen evolution activity for all synthesized Ti/SnO_2-Sb electrodes in comparison with Ti plate (Figure 4). Also, the comparative electrochemical behavior of doxorubicin (DOX) on all electrodes was studied by CV (Figure 5).

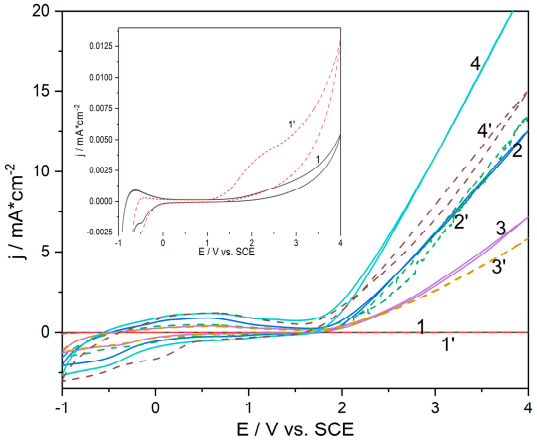

Preprints (www.preprints.org) | NOT PEER-REVIEWED | Posted: 31 May 2023 doi:10.20944/preprints202305.2190.v1

Figure 4. Comparative cyclic voltammograms recorded in 0.1 M Na_2SO_4 (solid line) and mixture of 0.05 M Na_2SO_4 with 0.05 M NaCl (dot line) supporting electrolyte at the electrodes: Ti plate (curves 1, 1′); Ti/SnSb-S0 (curves 2, 2′); Ti/SnSb-S1 (curves 3, 3′); Ti/SnSb-S2 (curves 4, 4′).

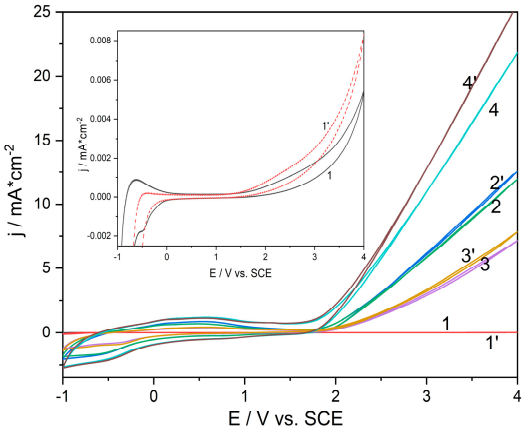

Figure 5. Comparative cyclic voltammograms recorded in 0.1 M Na_2SO_4 (solid line) and 5 mg·L^{-1} DOX (dot line) supporting electrolyte at the electrodes: Ti plate (curves 1, 1′); Ti/SnSb-S0 (curves 2, 2′); Ti/SnSb-S1 (curves 3, 3′); Ti/SnSb-S2 (curves 4, 4′).

The presence of Cl^- ion in the solution has a polarization effect for all Ti/SnO_2-Sb electrodes in contrast with Ti plate, for which a depolarization effect with a significant current increasing corresponding to chlorine generation is noticed (Figure 5). The presence of DOX exhibited a depolarization effect with current density increasing due to the DOX direct oxidation process occurring (Figure 5).

In addition to OERP, the oxygen evolution activity can be evaluated by the current density value that represent the oxygen evolution reaction rate, which is direct proportional with the amount of electric charge [36]. As shown in Figure 4, Ti plate exhibited the lowest OERP that is characteristic to the "active" electrodes [37] but with the very low current density in both capacitive component and Faradaic response for the oxygen evolution as reaction rate. Ti/SnSb-S2 electrode exhibited the highest current density and as consequence, the higher reaction rate, and the OERP value lower than the other Ti/SnSb electrodes but higher than Ti plate. This type of electrode is included in the "non-active" category of the electrode, but all dimensionally stable anode types electrode can have mixed behaviour during electrooxidation process, in according with the reactions (17)-(20) [38]:

$$MO_x + H_2O \rightarrow MO_x(HO\cdot) + H^+ + e^- \quad (17)$$

$$MO_x(HO\cdot) \rightarrow MO_{x+1} + H^+ + e^- \quad (18)$$

$$MO_{x+1} + R \rightarrow MO_x + RO \quad (19)$$

$$MO_x(HO\cdot) + R \rightarrow MO_x + CO_2 + H_2O + H^+ + e^- \quad (20)$$

3.3. Electrochemical oxidation of DOX

Electrooxidation was carried out at the constant potential through chronoamperometry (CA) running for one hour using all synthesized Ti/SnO_2-Sb electrodes. Chronoamperograms were recorded in both 0.1 M Na_2SO_4 solution and mixture of 0.05 M Na_2SO_4 and 0.05 M NaCl solution supporting electrolyte at the potential value of +3.0 V/SCE for the electrooxidation of 5 mg·L^{-1} DOX (Figure 6a). The highest current densities were recorded for Ti/SnSb-S2 electrode in both supporting electrolytes and the chloride ions decreases slightly the current densities, which is in accordance with the CVs results.

Also, the chronoamperometry was running at the potential value of +2.00, +3.00 and +4.00 V/SCE to determine the effect of the potential value on the DOX degradation and mineralization efficiency (Figure 6b). As it was expected, the current densities increased at higher potential value. Better

Preprints (www.preprints.org) | NOT PEER-REVIEWED | Posted: 31 May 2023 doi:10.20944/preprints202305.2190.v1

degradation and mineralization degrees were reached for the potential value of +3.00 V/SCE, which was considered the optimal one (the results are not shown here).

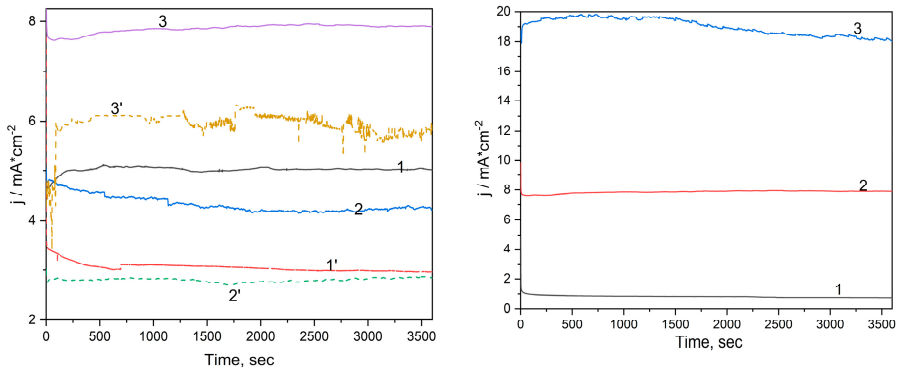

(a) (b)

Figure 6. (a)Time-evolution of chronoamperograms recorded at the potential value of +3.00 V vs SCE for electrooxidation of 5 mg·L^{-1} DOX in 0.1 M Na_2SO_4 (solid lines) and mixture of 0.05 M Na_2SO_4 with 0.05 M NaCl (dots lines) supporting electrolytes recorded with Ti/SnSb-S0 (curves 1, 1′); Ti/SnSb-S1 (curves 2, 2′); Ti/SnSb-S2 (curves 3, 3′); (b)Time-evolution of chronoamperograms recorded in 0.1 M Na_2SO_4 supporting electrolyte and 5 mg·L^{-1} DOX with Ti/SnSb-S2 electrode at the different potential values: +2.00 V vs SCE (curve 1), +3.00 V vs SCE (curve 2) and +4.00 V vs SCE (curve 3).

The DOX degradation and mineralization degrees reached at the potrential value of +3.00 V/SCE are gathered in Table 1, which presents also the OERP and the current densities for all tested electrodes. Ti/SnSb-S2 obtained after controlled corrosion with oxalic acid exhibited the lowest OERP and the highest current density as the reaction rate.

Table 1. OERP and DOX degradation/mineralization degrees achieved for all tested electrodes after one hour electrolysis time (C_{DOX}=5 mg·L^{-1}) at the potential value of +3.00 V/SCE (including current densities).

Electrode	Supporting electrolyte	E_{O_2} / V vs. SCE	Current densities, A/m^2	Mineralization degree (η_{TOC}), %	DOX degradation degree (η_{DOX}), %			
					λ = 486 nm	λ = 290 nm	λ = 253 nm	λ = 232 nm
Ti/SnSb-S0	0.1 M Na_2SO_4	1.75	22	5	70	23	12	9.5
	0.05 M Na_2SO_4 + 0.05 M NaCl	1.72	14	4	80	-*	9.4	7.07
Ti/SnSb-S1	0.1 M Na_2SO_4	1.80	29	16	90	44	64	67
	0.05M Na_2SO_4 + 0.05 M NaCl	1.77	31	28	93	-*	74	47
Ti/SnSb-S2	0.1 M Na_2SO_4	1.65	77	42	99	88	95	96
	0.05M Na_2SO_4 + 0.05 M NaCl	1.58	61	67	98	-*	98	87

*Could not be read due to chlorine discharge (see Figure 7c).

Preprints (www.preprints.org) | NOT PEER-REVIEWED | Posted: 31 May 2023 doi:10.20944/preprints202305.2190.v1

Also, the best degradation and mineralization degrees were achieved using Ti/SnSb-S2 electrode, which allowed a complete decolorization (λ = 486 nm) and high degradation of the methoxy group (λ = 232 nm), the aromatic ring and the quinonoid structure (λ = 253; 290 nm) [29]. This is supported also by Figure 7a that displays the comparative UV-VIS spectra recorded after one hour electrolysis using all three electrodes. Also, Ti/SnSb-S2 electrode accomplishes 42 % mineralization degree, while Ti/SnSb-S0 electrode was not able to mineralize DOX under tested conditions. The presence of chloride enhanced the overall performance of the electrode, but UV-VIS spectrum shape was modified through increasing absorbance at about wavelength of 290 nm due to increased concentration of hypochlorite during electrolysis (Figure 7b).

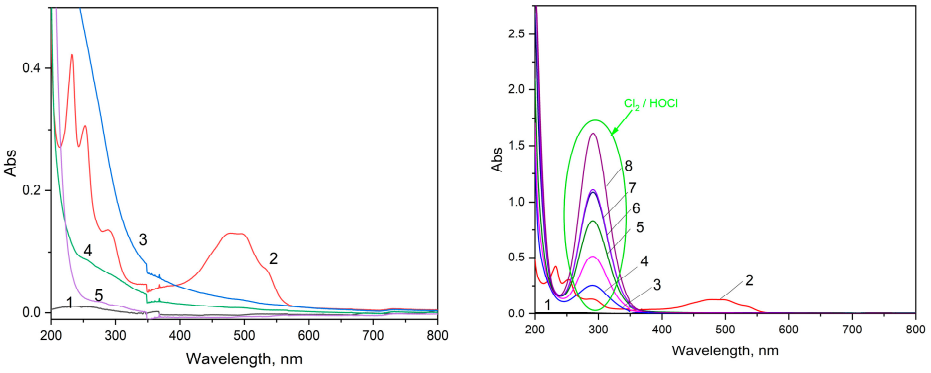

Figure 7. UV-VIS spectrum recorded for 5 mg·L^{-1} DOX (initial-curve 2) and after one hour electrolysis in 0.1M Na_2SO_4 supporting electrolyte at an applied potential of +3.0 V vs. SCE, using the electrodes: Ti/SnSb-S0 (curve 3); Ti/SnSb-S1 (curve 4); Ti/SnSb-S2 (curve 5) electrodes; (b)UV-VIS spectra recorded for 5 mg·L^{-1} DOX (initial-curve 2) and after different electrolysis time: 10; 20; 30; 60; 90 and 120 minutes (curves: 3 - 8) in 0.05 M Na_2SO_4 + 0.05 M NaCl supporting electrolyte, at an applied potential of 3.0 V vs. SCE.

Also, form the kinetics point of view, a comparative evaluation of the effect of both supporting electrolytes (0.1 M Na_2SO_4 and mixture of 0.05 M Na_2SO_4 and 0.05 M NaCl) on the mineralization current efficiencies determined based on equation (5) was followed and the results are gathered in Table 2. Also, the limiting current density (i_{lim}) and the mass transfer coefficient for mineralization (k_d) were determined based on equation (21) and respective, (22) [39]:

$$i_{lim} = z \cdot F \cdot k_d \cdot C_R \quad (21)$$

where: i_{lim} is limiting current density for organics mineralization (A·m^{-2}), z is the number of electrons involved in organics mineralization reaction, F is the Faraday constant (96.487 C· mol^{-1} , k_d is the mass transfer coefficient (m · s^{-1}) and C_R is the concentration of organics in the bulk solution (mol· m^{-3})

$$\frac{TOC}{TOC_0} = \exp\left(-\frac{A}{V} \cdot k_d \cdot t\right) \quad (22)$$

where: TOC_0 and TOC is the initial concentration of total organic carbon of compounds and at time t, respectively, A is the anodic active surface area (in m^2), V is the volume of the treated solution (in dm^3), k_d is the mass transport coeficient related to mineralization (m · s^{-1}) and t is the electrolysis time (seconds).

Preprints (www.preprints.org) | NOT PEER-REVIEWED | Posted: 31 May 2023 doi:10.20944/preprints202305.2190.v1

Table 2. Kinetics parameters and energy consuming-based efficacy for electrochemical oxidation of 5 mg·L^{-1} DOX at Ti/SnSb-S2 electrode in 0.1 M Na_2SO_4 and mixture of 0.05 M Na_2SO_4 and 0.05 M NaCl.

Supporting electrolyte	Time, (sec)	k_d, (m·s^{-1}) ·10^6	j_{lim}, A·m^{-2}	MCE, %	E_{TOC}, mg C/C·cm^2	W_{sp}, kWh·dm^{-3}	SEC, kWh·g^{-1} TOC removed
0.05 M Na_2SO_4+0.05 M NaCl	600	34.2	3.64	6.9	0.960	0.525	0.434
	1200			5.1	0.840	1.10	0.582
	1800			3.4	0.501	1.80	0.887
	3600			1.5	0.233	4.35	1.98
0.1 M Na_2SO_4	600	10.5	1.12	1.7	0.159	0.35	1.75
	1200			1.9	0.178	0.62	1.56
	1800			1.3	0.123	1.12	2.25
	3600			1.3	0.116	2.61	2.37

Considering the current densities corresponding to the applied potential value of +3.00 V/SCE (Table 1), it is obviously that the electrooxidation process occurred under the mass transfer control for all tested operation conditions of water discharge generating O_2 evolution involving hydroxyl radicals and other oxidants linked to the supporting electrolyte composition (*e.g.*, chlorine, in accordance with reactions (14) and (15)).

In comparison with our previously reported paper related to Ti/SnO_2 that allowed electrochemical DOX conversion without mineralization at the potential of +3.00 V/ESC [29], Ti/SnSb-S2 exhibited significant enhanced performance for DOX degradation and mineralization. Also, higher mineralization current efficiency was achieved in the presence of chloride due to a supplementary acting as oxidant of chlorine and other chlorine-based species. The electrochemical efficiency related to the DOX mineralization determined based on equation (4) showed better results in the presence of mixture of 0.05 M Na_2SO_4 and 0.05 M NaCl. Energy consuming reported per liter of the water treated is better in the absence of chloride, probably due to a part of the energy is consumed to generate chlorine, from which a main part is wasted.

3.4. Activated carbon-based sorption-assisted electrochemical oxidation of DOX using Ti/SnSb-S2

Considering the principles of the electrochemical filtration, 1 g·L^{-1} activated carbon, which is well-known as mature technology in water treatment technology, was added with the role of the particulate electrode in the electrochemical system using 0.1 M Na_2SO_4 supporting electrolyte and Ti/SnSb-S2 electrode. The results are presented in Table 3.

Table 3. Kinetics parameters and energy consuming-based efficacy for electrochemical oxidation of 5 mg·L^{-1} DOX using EF process in 0.1 M Na_2SO_4 supporting electrolyte.

Supporting electrolyte	Time, (sec)	k_d, (m·s^{-1}) ·10^6	j_{lim}, A·m^{-2}	MCE, %	E_{TOC}, mg C/C·cm^2	W_{sp}, Wh·dm^{-3}	SEC, Wh·g^{-1} TOC removed
0.1 M Na_2SO_4	600	19.1	2.03	7.1	0.980	0.515	0.420
	1200			5.5	0.870	1.05	0.610
	1800			6.5	0.518	1.32	0.840
	3600			5.6	0.590	3.25	1.16

It is obvious that the AC improved the process performance through mass transfer enhancement and the sorption of DOX in electrochemical system. Also, under the electric field application, AC particles can be converted into charged microelectrodes exhibiting the electro-sorption of DOX and the ability to degrade and mineralize adsorbed DOX [24–27].

Preprints (www.preprints.org) | NOT PEER-REVIEWED | Posted: 31 May 2023 doi:10.20944/preprints202305.2190.v1

Thus, the mechanism for DOX removal of pollutants in activated carbon-based sorption - assisted electrooxidation of DOX is very complex. The presence of activated carbon particulate electrode should influence the DOX degradation / mineralization mechanism through a potential sorbent role. The electrochemical reactions on the non-active anode should be similar to electrochemical oxidation [41]. The question that arises is related to the global effect of both processes regarding DOX degradation and mineralization. To elucidate these aspects, each process was applied individually for DOX removal trough sorption on AC (**S**), degradation and mineralization through both electrooxidation (**EO**) and activated carbon-based sorption-assisted electrooxidation (**EF**). The presence of activated carbon increased the diffusion constant related to mineralization, which is expected due to its presence in the solution bulk. Also, the limiting current density increased in the presence of the activated carbon. A great enhancement is noticed for the mineralization current efficiency (MCE). Moreover, synergic effect of the hybrid process of activated carbon - assisted electrooxidation (EF) is proved based on the kinetics constants expressed as $\ln(C_0/C_t) = k(t)$ considering the pseudo-first-order model that fit well (correlation coefficient > 0.9) for each individual and hybrid process (Table 4) using equation (23):

$$\text{Synergy (\%)} = \frac{k_{EF} - k_{EO} - k_S}{k_{EF}} \cdot 100 \quad (23)$$

where k_{EF}, k_{EO}, k_S are the kinetic coefficient of pollutant removal in EF, the electrochemical degradation system without AC and the sorption AC system.

The synergy in EF process of 52.75 % was calculated for TOC parameter removal. This is in accordance with the literature [42,43] reported for various configuration of GAC sorption assisted electrooxidation using different DSA-type anodes and higher than the one reported for greywater treatment by Garcia et al, 2018 [44]. The presence of activated carbon under the electric field between anode and cathode within undivided cell assure creating a double electric layer that is able to adsorb organic pollutant by electro sorption mechanism [45]. Also, AC particles are polarized as anode and as cathode depending on their position generating a large number of micro-electrolysis cells, which should generate oxidant species (*e.g.*, hydroxyl radicals) able to oxidize and mineralize the organic pollutant adsorbed onto its surface [26,46].

For the EO and EF processes, the apparent rate was determined using relation $\ln(C_0/C_t) = k'_E(C)$, in which C represents the electrical charge passed during EO and EF processes applied for DOX degradation and mineralization [47]. The results gathered in Table 4 shows the superiority of EF in comparison with EO (2.72 vs 0.555 C^{-1}), regarding the mineralization process.

The effective mineralization rate assessed as the ratio between the apparent mineralization rate constant calculated for the TOC analysis and the apparent degradation rate constant calculated based on UV analysis ($k'_{E,TOC}$ / $k'_{E,UV}$) [47] showed the superiority of EF ($k'_{E,TOC}$ / $k'_{E,UV}$ = 0.90) in comparison with EO ($k'_{E,TOC}$ / $k'_{E,UV}$ = 0.12).

Table 4. Kinetics coefficients are determined for each process using pseudo-first order model.

Process	Parameter	k, min^{-1}	R^2	k'_E, C^{-1}	R^2
S	λ_{DOX} = 486nm	0.004	0.937	-	-
	λ_{DOX} = 290nm	0.0011	0.911	-	-
	λ_{DOX} = 253nm	0.0018	0.969	-	-
	λ_{DOX} = 232nm	0.0015	0.966	-	-
	TOC, $mg \cdot L^{-1}$	0.0011	0.95	-	-
EO	λ_{DOX} = 486nm	0.07	0.998	4.724	0.99
	λ_{DOX} = 290nm	0.02	0.999	1.524	0.999
	λ_{DOX} = 253nm	0.034	0.999	2.535	0.999
	λ_{DOX} = 232nm	0.032	0.999	2.545	0.999
	TOC, $mg \cdot L^{-1}$	0.0084	0.96	0.555	0.999
EF	λ_{DOX} = 486nm	0.04	0.976	3.01	0.993
	λ_{DOX} = 290nm	0.02	0.952	0.55	0.944

Preprints (www.preprints.org) | NOT PEER-REVIEWED | Posted: 31 May 2023 doi:10.20944/preprints202305.2190.v1

λ_{DOX} = 253nm	0.021	0.967	1.461	0.998
λ_{DOX} = 232nm	0.023	0.966	1.624	0.991
TOC, mg·L^{-1}	0.02	0.900	2.721	0.986

The synergic effect of the combination of electrooxidation and sorption processes operating at high voltage may be attributed to both indirect and direct electrochemical oxidation of DOX improving the transfer stage by DOX sorption onto AC and its further oxidation by the direct transfer of electrons and by hydroxyl radicals generated at the Ti/SnSb-S2 electrode surface and AC microanodes.

Considering the results related to the rate constants for DOX degradation and mineralization by EO using Ti/SnSb-S2 electrode, the tendency is similar to that reported by our group for DOX degradation using 3-D Ti/SnO_2 [29]. However, better mineralization current efficiency was achieved using Ti/SnSb-S2 electrode due to its better electrochemical activity for radicals generation. The degradation and mineralization process imply by the electron transfer at the solution-electrode surface interface that assured the DOX decolorization as direct electrolysis followed by the attack the hydroxyl radicals and/or other oxidants (*e.g.*, Cl_2) generated and adsorbed on the electrode surface through their diffusion into the bulk solution in according with the reactions (24,25):

$$H_2O + Ti/SnSb - S_2 \rightarrow Ti/SnSb - S_2(\cdot OH) + H^+ + e^- \quad (24)$$

$$Ti/SnSb - S_2(\cdot OH) + C_{27}H_{29}NO_{11} + 46H_2O \rightarrow Ti/SnSb - S_2 + 27CO_2 + 121H^+ + NO_3^- + 120e^- \quad (25)$$

The presence of AC as EF process complicates more the mechanism considering the reduction of the O_2 as H_2O_2 that generates the hydroxyl radicals acting in mineralization process of DOX adsorbed onto AC surface in according with reactions (26, 27):

$$O_2 + 2H^+ + 2e^- \rightarrow AC(H_2O_2) \rightarrow AC(\cdot OH) \quad (26)$$

$$AC(\cdot OH) + C_{27}H_{29}NO_{11} + 46H_2O \rightarrow AC + 27CO_2 + 121H^+ + NO_3^- + 120e^- \quad (27)$$

This mechanism is proved by the above-discussed kinetics aspects presented in Table 4 and explains the synergic effect of the combination of EO with S process into EF one.

3.5. Comparative simultaneous mineralization of DOX, capecitabine (CCB) and humic acid (HA) by EO and EF

Considering the common presence of humic acid (HA) as main component of natural organic matter in surface water and the potential presence of other cytostatic such as capecitabine (CCB), Ti/SnSb-S2-based EO was tested for each individual pollutant (5 mg·L^{-1} DOX, 5 mg·L^{-1} CCB and 10 mg·L^{-1} HA) and for their mixture (5 mg·L^{-1} DOX + 5 mg·L^{-1} CCB + 10 mg·L^{-1} HA) mineralization. The activated carbon-based sorption-assisted electrochemical oxidation using Ti/SnSb-S2 (EF) process was tested for the same mixture composition. The UV-VIS spectra recorded for initial solutions and after treatment by EO are shown in Supplementary materials, Figure S2.

The degradation of each pollutant occurred by EO. Also, the degradation of the mixture is proved by UV-VIS spectra using both EO and EF. Mineralization degrees, electrochemical efficiencies, and mineralization current efficiencies for each pollutant and for their mixture are presented in Figure 8.

Preprints (www.preprints.org) | NOT PEER-REVIEWED | Posted: 31 May 2023 doi:10.20944/preprints202305.2190.v1

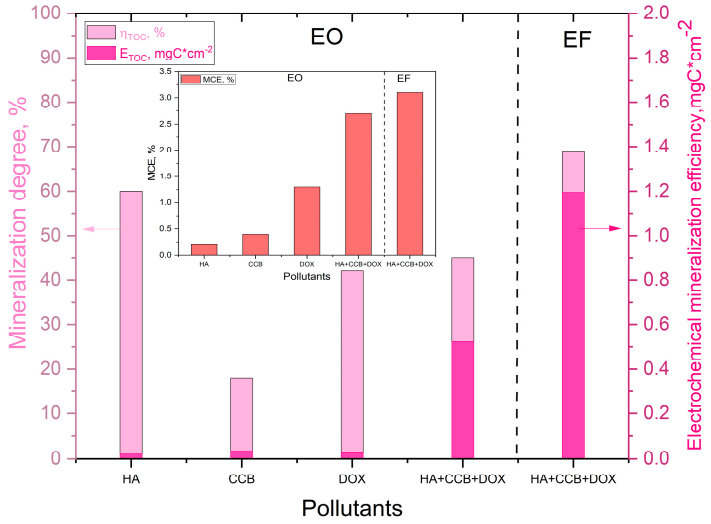

Figure 8. The comparative mineralization degrees and electrochemical mineralization efficiency of Ti/SnSb-S2 electrode after one hour of chronoamperometry running at +3.00 V/SCE in 0.1 M Na_2SO_4 supporting electrolyte for different individual pollutants (DOX, CCB, HA) and their mixture in the absence and the presence of 1 g·L^{-1} AC; Inset: Mineralization current efficiency determined for similar operating conditions.

It is obviously an enhanced efficiency for EF in comparison with EO. Also, better efficacy in terms of the energy consumed per g of TOC is provided by EF in comparison with EO. SEC of 0.653 kWh·g^{-1} TOC was determined for EF in comparison with 1.128 kWh·g^{-1} TOC for EO. These results clarify the superiority of EF for enhanced removal of mixture of the pollutants.

4. Conclusions

The controlled corrosion of the Ti plate under acidic medium using hydrofluoric acid and oxalic acid allowed to get mesoporous Sb-doped SnO_2 deposited onto Ti by spin-coating method. A more uniform deposition of Sb-doped SnO_2 with mitigate the "mud-like cracks" was achieved by controlled corrosion of the Ti substrate in comparison with uncorroded Ti plate.

Sb-doped SnO_2 deposited onto Ti plate corroded with oxalic acid, named Ti/SnSb-S2 electrode, exhibited the lowest potential value and the highest rate for oxygen evolution reaction. The best mineralization efficiency was achieved for doxorubicin (DOX) mineralization using Ti/SnSb-S2 electrode at the potential value of +3.00 V/SCE. The presence of Cl^- in supporting electrolyte enhanced the mineralization efficiency in the presence of Cl^-, 67 % vs 42 % in the absence of Cl^-. Energy consuming reported per liter of the water treated is mitigate in the absence of chloride, probably due to a part of the energy is consumed to generate chlorine, from which a main part is wasted, while the reduced energy consuming reported to the removed TOC was achieved.

The presence of activated carbon within the electrolysis process increased the mass transport enhancing the global mineralization process. Also, the mineralization current efficiency was improved substantially, and the effective mineralization was proved considering apparent mineralization rate constant reported to the apparent degradation mineralization constant. Moreover, a synergic effect was proved considering the kinetics aspects of all electrooxidation, sorption and activated carbon-assisted electrooxidation named electrochemical filtering processes. A synergy of 52.75 % was determined for TOC parameter removal, which is in accordance with the result reported by [44–46].

The mechanism of DOX degradation and mineralization is very complex involving both direct and indirect electrolysis generating hydroxyl radicals and other oxidants (*e.g.*, Cl_2 in the presence of Cl^-) at mesoporous Sb-doped SnO_2 deposited onto Ti plate corroded controlled with oxalic acid. In

Preprints (www.preprints.org) | NOT PEER-REVIEWED | Posted: 31 May 2023 doi:10.20944/preprints202305.2190.v1

addition, activated carbon micro-electrolysis cells configurated under applied voltage enhanced the hydroxyl radicals concentration with the consequence of the improved general process performance.

The superiority of EF was proved considering simultaneous degradation and mineralization of mixture of doxorubicin, capecitabine and humic acid, which shows the great potential of the hybrid process to be used in advanced treatment of water.

Supplementary Materials: The following supporting information can be downloaded at the website of this paper posted on Preprints.org. Figure S1: UV-VIS spectra in 0.1M Na_2SO_4 supporting electrolyte and in the presence of different initial pollutants: 5mg·L^{-1} DOX (curve 1), 5mg·L^{-1} CCB (curve 2), and 10mg·L^{-1} HA (curve 3), Figure S2: UV-VIS spectra in 0.1M Na_2SO_4 supporting electrolyte, in the presence of an initial mixture of 5 mg·L^{-1} DOX, 5 mg·L^{-1} CCB and 10 mg·L^{-1} HA (curve 1) and after treatment by EO (curve 2), and after treatment by EF (curve 3) at an applied potential of +3.00 V vs. SCE.

Author Contributions: F.M.; methodology, F.M and C.O; investigation, A.B., R.N., C.O., M.N., S.I.; writing—original draft preparation, F.M., C.O., A.B.; writing—review and editing, F.M. and A.B.; supervision, F.M.; All authors have read and agreed to the published version of the manuscript." Please turn to the CRediT taxonomy for the term explanation. Authorship must be limited to those who have contributed substantially to the work reported.

Funding: This research received no external funding

Institutional Review Board Statement: Not applicable

Data Availability Statement: Not applicable.

Acknowledgments: This work was supported partially by a grant of the Romanian Ministry of Education and Research, "Program intern de stimulare si recompensare a activitatii didactice", contract number 10161/11 June 2021.

Conflicts of Interest: The authors declare no conflict of interest.

References

1. Sirés, I.; Brillas, E. Remediation of water pollution caused by pharmaceutical residues based on electrochemical separation and degradation technologies: A review. *Environ Int* **2012**, *40*, 212–229, https://doi.org/10.1016/j.envint.2011.07.012.
2. Oturan, M.A.; Aaron, J.J. Advanced oxidation processes in water/wastewater treatment: Principles and applications. A review. *Crit Rev Environ Sci Technol* **2014**, *44*, 2577–2641, https://doi.org/10.1080/10643389.2013.829765.
3. Awad, Y.M.; Abuzaid, N. Electrochemical oxidation of phenol using graphite anodes. *Sep Sci Technol* **1999**, *34*, 699–708. https://doi.org/10.1081/SS-100100675.
4. Montilla, F.; Morallón, E.; Vázquez, J.L. Electrochemical study of benzene on Pt of various surface structures in alkaline and acidic solutions. *Electrochim Acta* **2002**, *47*, 4399–4406, https://doi.org/10.1016/S0013-4686(02)00520-0.
5. Montilla, F.; Michaud, P.A.; Morallón, E.; Vázquez, J.L.; Comninellis, Ch. Electrochemical oxidation of benzoic acid at boron-doped diamond electrodes. *Electrochim Acta* **2002**, *47*, 3509–3513, https://doi.org/10.1016/S0013-4686(02)00318-3.
6. Trasatti, S. Electrocatalysis: understanding the success of DSA. *Electrochim Acta* **2000**, *45*, 2377-2385, https://doi.org/10.1016/S0013-4686(00)00338-8.
7. Kariman, A.; Marshall, A.T. Improving the stability of DSA electrodes by the addition of TiO_2 nanoparticles. *J Electrochem Soc* **2019**, *166*, E248-E251, 10.1149/2.0761908jes.
8. Cao, F.; Tan, J.; Zhang, S.; Wang, H.; Yao, C.; Li, Y. Preparation and recent developments of Ti/SnO_2-Sb Electrodes. *J Chem Hindawi* **2021**, *2021*, 1-13, https://doi.org/10.1155/2021/2107939.
9. Ruparelia, J.P.; Soni, B.D. Application of Ti/RuO_2-SnO_2-Sb_2O_5 anode for degradation of reactive black-5 dye. *Int Schol Sci Res Innov* **2012**, *6*, 715-721, doi.org/10.5281/zenodo.1070603.
10. Machado, C.F.C.; Gomes, M.A.; Silva, R.S.; Salazar-Band, G.R.; Eguiluz, K.I.B. Time and calcination temperature influence the electrocatalytic efficiency of Ti/SnO_2: Sb (5%), Gd(2%) electrodes towards the electrochemical oxidation of naphthalene. *J Electroanal Chem* **2018**, *816*, 232–241, https://doi.org/10.1016/j.jelechem.2018.03.053.
11. Shao, D.; Li, X.; Xu, H.; Yan, W.A. Simply improved Ti/Sb-SnO_2 electrode with stable and high performance in electrochemical oxidation process. *RSC Adv* **2014**, *4*, 21230-21237, doi https://doi.org/10.1039/C4RA01990C.
12. Maharana, D.; Niu, J.; Gao, D.; Xu, Z.; Shi, J. Electrochemical degradation of rhodamine B over Ti/SnO_2-Sb electrode. *Water Environ Res* **2015**, *87*, 304–311. https://doi.org/10.2175/106143015X14212658613514.

Preprints (www.preprints.org) | NOT PEER-REVIEWED | Posted: 31 May 2023 doi:10.20944/preprints202305.2190.v1

13. Zhang, S.; Chen, X.; Du, S.; Wang, J.; Tan, M.; Dong J.; Wu, D. Facile synthesis of highly active Ti/Sb-SnO_2 electrode by sol-gel spinning technique for landfill leachate treatment. *Water Sci Technol* **2021**, *84*, 1366–1378. https://doi.org/10.2166/wst.2021.336.
14. Zhang, Y.; Yang, Y.; Yang, S.; Quispe-Cardenas, E.; Hoffmann, M.R. Application of heterojunction Ni–Sb–SnO_2 anodes for electrochemical water treatment, *ACS EST Engg* **2021**, *1*, 1236-1245, https://doi.org/10.1021/acsestengg.1c00122.
15. Zhou, C.; Wang, Y.; Chen, J.; Xu, L.; Huang, H.; Niu, J. High-efficiency electrochemical degradation of antiviral drug abacavir using a penetration flux porous Ti/SnO_2–Sb anode. *Chemosphere* **2019**, *225*, 304–310, https://doi.org/10.1016/j.chemosphere.2019.03.036.
16. Sun, Y.; Cheng, S.; Mao, Z.; Lin, Z.; Ren, X.; Yu, Z. High electrochemical activity of a Ti/SnO_2–Sb electrode electrodeposited using deep eutectic solvent. *Chemosphere* **2020**, *239*, 124715, https://doi.org/10.1016/j.chemosphere.2019.124715.
17. Sivakumar, P.; Akkera, H.S.; Kumar Reddy, T.R.; Bitla, Y.; Ganesh, V.; Kumar, P.M.; Reddy, G.S.; Poloju, M. Effect of Ti doping on structural, optical, and electrical properties of SnO_2 transparent conducting thin films deposited by sol-gel spin coating. *Opt Mater* **2021**, *113*, 110845, https://doi.org/10.1016/j.optmat.2021.110845.
18. Elangovan, E.; Shivashankar, S.A.; Ramamurthi, K. Studies on structural and electrical properties of sprayed SnO_2: Sb films. *J Cryst Growth* **2005**, *276*, 215–22, https://doi.org/10.1016/j.jcrysgro.2004.11.387.
19. Ma, J.; Gao, M.; Shi, H.; Ni, J.; Xu, Y.; Wang, Q.; Progress in research and development of particle electrodes for three-dimensional electrochemical treatment of wastewater: A review. *Environ Sci Pollut R* **2021**, *28*, 47800-47824, https://doi.org/10.1007/s11356-021-13785-x.
20. Zhang, C.; Jiang, Y.; Li, Y.; Hu, Z.; Zhou, L. Zhou, M. Three-dimensional electrochemical process for wastewater treatment: A general review. *Chem Eng J* **2013**, *228*, 455-467, https://doi.org/10.1016/j.cej.2013.05.033.
21. Gedam, N.; Neti, N.R. Carbon attrition during continuous electrolysis in carbon bed based three-phase three-dimensional electrode reactor: treatment of recalcitrant chemical industry wastewater. *J Environ Chem Eng* **2014**, *2*, 1527–1532, https://doi.org/10.1016/j.jece.2014.06.025.
22. Alighardashi, A.; Aghta, R.S.; Ebrahimzadeh, H. Improvement of carbamazepine degradation by a three-dimensional electrochemical (3-EC) process. *Int J Environ Res* **2018**, *12*, 451–458, https://doi.org/10.1007/s41742-018-0102-2.
23. Lei, S.; Song, Y. Comparative study on electrochemical treatment of cyanide wastewater. *Front Chem* **2021**, *9*, 598228, 10.3389/fchem.2021.598228.
24. Sowmiya, S.; Gandhimathi, R.; Ramesh, S.T.; Nidheesh, P.V. Granular activated carbon as a particle electrode in three-dimensional electrochemical treatment of reactive black b from aqueous solution. *Environ Prog Sustain* **2016**, *35*, 1616-1622, https://doi.org/10.1002/ep.12396.
25. McQuillan, R.V.; Stevens, G.W.; Mumford K.A. The electrochemical regeneration of granular activated carbons: A review. *J Hazard Mater* **2018**, *355*, 34-49, https://doi.org/10.1016/j.jhazmat.2018.04.079.
26. Norra, G.F.; Radjenovic, J. Removal of persistent organic contaminants from wastewater using a hybrid electrochemical-granular activated carbon (GAC) system. *J Hazard Mater* **2021**, *415*, 125557, https://doi.org/10.1016/j.jhazmat.2018.04.079.
27. Zhan, J.; Li, Z.; Yu, G.; Pan, X.; Wang, J.; Zhu, W.; Han, X.; Wang, Y. Enhanced treatment of pharmaceutical wastewater by combining three-dimensional electrochemical process with ozonation to in situ regenerate granular activated carbon particle electrodes. *Sep Purif Technol* **2019**, 208, 12-18, https://doi.org/10.1016/j.seppur.2018.06.030.
28. Neti, N.R.; Misra, R. Efficient degradation of Reactive Blue 4 in carbon bed electrochemical reactor. *Chem Eng J* **2012**, *184*, 23–32, https://doi.org/10.1016/j.cej.2011.12.014.
29. Orha, C.; Bandas, C.; Lazau, C.; Popescu, M.I.; Baciu, A.; Manea, F. Advanced electrodegradation of doxorubicin in water using a 3-D Ti/SnO_2 anode. *Water* **2022**, *14*, 821 https://doi.org/10.3390/w14050821.
30. Comninellis, Ch.; Pulgarin, C. Anodic oxidation of phenol for wastewater treatment. *J Appl Electrochem* **1991**, *21*, 703–708, https://doi.org/10.1007/BF01034049.
31. Yang, B.; Wang, J.; Jiang, C.; Li, J.; Yu, G.; Deng, S.; Lu, S.; Zhang, P.; Zhu, C.; Zhuo, Q. Electrochemical mineralization of perfluorooctane sulfonate by novel F and Sb co-doped Ti/SnO_2 electrode containing Sn-Sb interlayer. *Chem Eng J* **2017**, *316*, 296–304, https://doi.org/10.1016/j.cej.2017.01.105.
32. Bi, Q.; Guan, W.; Gao, Y.; Cui, Y.; Ma, S.; Xue, J. Study of the mechanisms underlying the effects of composite intermediate layers on the performance of Ti/SnO_2-Sb-La electrodes. *Electrochim Acta* **2019**, *306*, 667–679, https://doi.org/10.1016/j.electacta.2019.03.122.
33. Li, D.; Liu H.; Feng L. A review on advanced FeNi-based catalysts for water splitting reaction. *Energ Fuel* **2020**, *34*, 13491–13522. https://doi.org/10.1021/acs.energyfuels.0c03084.
34. Li, J.; Li, Mo.; Li, D.; Wen, Q.; Chen Z. Electrochemical pretreatment of coal gasification wastewater with Bi-doped PbO_2 electrode: Preparation of anode efficiency and mechanism. *Chemosphere* **2020**, *248*, 126021, https://doi.org/10.1016/j.chemosphere.2020.126021.

Preprints (www.preprints.org) | NOT PEER-REVIEWED | Posted: 31 May 2023 doi:10.20944/preprints202305.2190.v1

35. Li, X.; Yan, J.; Zhu, K. Effects of IrO_2 interlayer on the electrochemical performance of Ti/Sb-SnO_2 electrodes. *J Electroanal Chem* **2020**, *878*, 114471, https://doi.org/10.1016/j.jelechem.2020.114471.
36. Guo, H.; Xu, Z.; Wang, D.; Chen, S.; Qiao, D.; Wan, D.; Xu, H.; Yan, W.; Jin, X. Evaluation of diclofenac degradation effect in "active" and "non-active" anodes: A new consideration about mineralization inclination. *Chemosphere* **2022**, *286*, 131580, https://doi.org/10.1016/j.chemosphere.2021.131580.
37. Martinez-Huitle, C.A.; Brillas, E. Decontamination of wastewaters containing synthetic organic dyes by electrochemical methods: A general review. *Appl Catal B Environ* **2009**, 87,105-145, https://doi.org/10.1016/j.apcatb.2008.09.017.
38. Panizza, M.; Cerisola, G. Direct and mediated anodic oxidation of organic pollutants. *Chem Rev* **2009,** *109*, 6541-6569, https://doi.org/10.1021/cr9001319.
39. Chin, C.J.M.; Chen, T.Y.; Lee, M.; Chang, C.F.; Liu, Y.T.; Kuo, Y.T. Effective anodic oxidation of naproxen by platinum nanoparticles coated FTO glass, *J Hazard Mater* **2014**, *277*, 110-119, https://doi.org/10.1016/j.jhazmat.2014.02.034.
40. Panizza, M.; Michaud, P.A.; Cerisola, G.; Comninellis, Ch. Anodic oxidation of 2-naphthol at boron-doped diamond electrodes. *J Electroanal Chemistry* **2001**, *507*, 206-214, https://doi.org/10.1016/S0022-0728(01)00398-9.
41. Zhu, X.; Ni, J.; Xing, X.; Li, H.; Jiang, Y. Synergies between electrochemical oxidation and activated carbon adsorption in three-dimensional boron-doped diamond anode system. *Electrochim Acta* **2011**, *56*, 1270–1274, https://doi.org/10.1016/j.electacta.2010.10.073.
42. Asgari, G.; Seid-mohammadi, A.; Rahmani, A.; Samadi, M. T.; Salari, M.; Alizadeh, S.; Nematollahi, D. Diuron degradation using three-dimensional electro-peroxone (3D/E-peroxone) process in the presence of TiO_2/GAC: Application for real wastewater and optimization using RSM-CCD and ANN-GA approaches. *Chemosphere* **2021**, *266*, 129179, https://doi.org/10.1016/j.chemosphere.2020.129179.
43. Samarghandi, MR.; Dargahi, A.; Rahmani, A.; Shabanloo, A.; Ansari, A.; Nematollahi, D. Application of a fluidized three-dimensional electrochemical reactor with Ti/SnO_2–Sb/β-PbO_2 anode and granular activated carbon particles for degradation and mineralization of 2,4-dichlorophenol: Process optimization and degradation pathway. *Chemosphere* **2021**, *279*, 130640, *https://doi.org/10.1016/j.chemosphere.2021.130640.*
44. García, E.A.; Agullo-Barcelo, M.; Bond, P.; Keller, J.; Gernjak, W.; Radjenovic, J. Hybrid electrochemical-granular activated carbon system for the treatment of greywater. *Chem Eng J* **2018**, *352*, 405-411, https://doi.org/10.1016/j.cej.2018.07.042.
45. Wang, T.; Song, Y.; Ding, H.; Liu, Z.; Baldwin, A.; Wong, I.; Li, H.; Zhao, C. Insight into synergies between ozone and in-situ regenerated granular activated carbon particle electrodes in a three-dimensional electrochemical reactor for highly efficient nitrobenzene degradation, *Chem Eng J* **2020**, *394*, 124852, https://doi.org/10.1016/j.cej.2020.124852.
46. Ghanbarlou, H.; Pedersen, N.L.; Fini, M.N.; Muff, J. Synergy optimization for the removal of dye and pesticides from drinking water using granular activated carbon particles in a 3D electrochemical reactor. *Environ Sci Pollut Res* **2020**, *27*, 22206-22213, https://doi.org/10.1007/s11356-020-08022-w.
47. Ratiu, C.; Manea, F.; Lazau, C.; Grozescu, I.; Radovan, C.; Schoonman, J. Electrochemical oxidation of p-aminophenol from water with boron-doped diamond anodes and assisted photocatalytically by TiO_2-supported zeolite, *Desalination* **2010**, *260*, 51–56, https://doi.org/10.1016/j.desal.2010.04.068.

Disclaimer/Publisher's Note: The statements, opinions and data contained in all publications are solely those of the individual author(s) and contributor(s) and not of MDPI and/or the editor(s). MDPI and/or the editor(s) disclaim responsibility for any injury to people or property resulting from any ideas, methods, instructions or products referred to in the content.